FR8500212

Université Scientifique et Médicale de Grenoble

INSTITUT DES SCIENCES NUCLÉAIRES
DE GRENOBLE

53, avenue des Martyrs · GRENOBLE

ISN 84.20
Mars 1984

CLASSICAL PROPERTIES AND SEMICLASSICAL QUANTIZATION OF A SPHERICAL NUCLEAR POTENTIAL

J. Carbonell, F. Brut, R. Arvieu
Institut des Sciences Nucléaires, Grenoble

J. Touchard
Division de Physique Théorique, Institut de Physique Nucléaire, Orsay

Submitted for publication

Laboratoire associé à l'Institut National de Physique Nucléaire et de Physique des Particules

CLASSICAL PROPERTIES AND SEMICLASSICAL QUANTIZATION

OF A SPHERICAL NUCLEAR POTENTIAL

J. CARBONELL, F. BRUT, R. ARVIEU

Institut des Sciences Nucléaires, 38026 Grenoble Cédex, France

and

J. TOUCHARD

Division de Physique Théorique, Institut de Physique Nucléaire

91406 Orsay Cedex, France.

CLASSICAL PROPERTIES AND SEMICLASSICAL QUANTIZATION OF A SPHERICAL NUCLEAR POTENTIAL

Abstract . The geometrical properties of the classical energy-action surface are studied for a nuclear Woods-Saxon-like spherical potential, in connection with the E.B.K. semiclassical method of quantization. Comparisons are made with other well known cases : the spherical harmonic oscillator and the spherical billiard. The shift of single particle energies from A = 208 to A = 16 is calculated by a simple method inspired by the Erhenfest adiabatic invariants. Semiclassical results are then compared with exact Schrödinger energies. It is seen that the most significant features of the single particle spectrum are explained by local properties of the energy action surface (curvature, slope) and by their evolution with the particle number.

1 . Introduction

The aim of this series of papers is to analyse in detail the classical dynamics of a particle in the average field of a nucleus which will be taken as spherical in the present article, then deformed in next papers and to draw as far as possible the relation between this dynamics and the quantum mechanical spectrum. There has been a revival of interest for semiclassical methods in the last decade which was partly oriented by the progress on the classical theory of dynamical systems (Percival 1977 and Berry 1981). In nuclear physics the efforts have been concentrated either on the understanding of shell effects by a method developed by several authors (Strutinsky 1967,1968,1974, Balian and Bloch 1970,1972,1974, Gutzwiller 1967,1971) or to mean properties by approximating the Hartree-Fock or the T.D.H.F. density matrix (see for example Schuck 1983). Although the energy levels of the nuclear average field have been calculated for many years by solving the Schrödinger equation and compared to experiments (Green et al. 1968), there has been little effort to connect them to classical trajectories by the W.K.B. or E.B.K. semiclassical method. The most recent discussion (Bohr and Mottelson 1975) is oriented mainly on the spirit of Strutinsky 1967, 1968,1974, Balian and Bloch 1970,1972,1974, Gutzwiller 1967,1971 . The E.B.K. method has the advantage that there is a one to one correspondence between one eigenstate and the classical trajectory which fulfill the quantum conditions. These particular orbits are embedded into the continuum of their neighbours. In most of the EBK calculations this embedding is not paid a particular attention : a spectrum is extracted and compared to experiment or to the exact wave mechanical solution and the differences, if any, are discussed. The E.B.K. method is potentially more powerful if one considers the set of all the possible trajectories. The purpose of this paper is to push as far as possible

the explanation of the energy levels by classical mechanics, in complete agreement with the old quantum mechanics.

The process of deforming the potential produces a deep change if the motion of the particle is treated classically. Indeed the one particle hamiltonian has the proper number of constants of motion to be classically integrable in the spherical version. In the deformed case the rotational invariance is lost; it is then questionable to find new constants of motion to replace the angular momentum. In two extreme cases : the harmonic oscillator and the ellipsoidal billiard (Berry 1981) this new constant is found to exist. In a preliminary work (Carbonell 1983 and Carbonell and Arvieu 1983) it has been shown that the nuclear potential shares with many dynamical systems (the Henon-Heiles system (see Henon and Heiles 1964), various deformed billiards (Berry 1981), the anisotropic Kepler problem (Gutzwiller 1982), electron in a Coulomb field superposed to a magnetic field (Robnik 1981) etc...)) the property to be non integrable. The direct connection between classical trajectories and quantum states is not possible everywhere then (Einstein 1917). Due to KAM theorem (Henon 1981) many quasiperiodic trajectories still exist and can be quantized (Noid et al. 1981). However the organization of the phase space becomes very complex (Heinon and Heiles 1964) : there are bifurcations of periodic trajectories (Bountis 1981), preserved tori, separatrices, destroyed tori and finally chaotic orbits (Henon 1981). When there is no macroscopic chaos the question arises to find in which topology (Reinhardt 1982) the actions may take the proper magnitude and to follow the proper tori as a function of deformation. Eventually the topology of the trajectories changes with the parameters (energy, deformation, size of the nucleus). The occurrence of the macroscopic chaos and its extension marks the limit of the E.B.K. semiclassical method.

This series of paper is thus intended to compare two situations : the integrable spherical potential in which the topology of the trajectory

is monotonous from one hand, the non integrable deformed potential in which the classical phase space has a highly complex structure from another hand. In this first paper we will concentrate on the study of the shape of a very important surface; the energy-action surface, which carries with it all the relevant information upon all classical trajectories. We will describe first model cases, the spherical harmonic oscillator, the spherical billiard,then a modified version of a spherical Woods-Saxon potential. Using a method similar to Erhenfest adiabatic invariants the one particle spectrum of all the nuclei considered as spherical is studied. The deviations of the surface from that of the model cases explain all the properties of the bound levels. The occurrence of the classical resonances is also discussed.

In a further publication the objective will be to describe the gross structure of the organization of the phase space in a deformed nucleus (Carbonell 1983 and Carbonell and Arvieu 1983) and the E.B.K. method will be pushed to its extreme limit by quantizing the available tori, if any.

2 . The energy-action surface

1 . The actions

Let us briefly remind the properties of spherical potentials. The Hamiltonian is written in obvious notations as

$$H = \frac{p_r^2}{2m} + \frac{\ell_c^2}{2m\, r^2} + V(r) \qquad (1)$$

The radial phase space for a given value of the classical angular momentum ℓ_c is obtained by considering the intersection of the energy surface with the (r,p_r) plane. The radial action I_r of a given trajectory is

the area defined by the integral

$$I_r = \frac{1}{2\pi} \oint_{C_r} p_r(E,\ell_c)\, dr = \frac{1}{2\pi} \oint_{C_r} \sqrt{2m\,(E-V(r)-\frac{\ell_c^2}{2m\,r^2})}\, dr \qquad (2)$$

in which C_r means a complete cycle of radial motion. Since the motion is partially degenerate (Goldstein 1980) for a spherical potential in spherical coordinates H depends on the two other actions I_θ , I_ϕ through $I_\theta + I_\phi$ and moreover it is known (Goldstein 1980) that

$$I_\theta + I_\phi = \ell_c \qquad (3)$$

For integrable systems H depends only upon the actions and is written as

$$H = H\,(I_r,\ \ell_c) \qquad (4)$$

Every orbit of a spherical potential is represented by a point in a three dimensional space with coordinate E, I_r, ℓ_c. By spanning every initial condition the point describes a surface : the energy-action surface, which characterizes the dynamical system under study.

The energy-action surface of the diffuse potential defined in section 3 - 1 below is represented on fig. 1 for A = 16, A = 90 and A = 208. Its properties will be described in detail in section 4.

In the following the set of curves $p_r(E,\ell_c)$ indexed by ℓ_c which express p_r as a function of r at a given energy are drawn for the diffuse potential (fig. 2). Two values of ℓ_c play an important role : $\ell_c = 0$ and $\ell_{c\,max}$. The trajectory with $\ell_c = 0$ has the highest possible p_r for a given r and marks the limit of the extension of the radial phase space at given E. On the other hand the trajectory with ℓ_{cmax} has $p_r = 0$ and is represented by a point. The lowest the ℓ the most "peripheral"

is the trajectory in the radial phase space. The set of curves $\{r,p_r\}$ can be interpreted as well as Poincaré surfaces of section which are popular in the theory of dynamical systems (Henon, 1981).

2 . Quantization conditions

Although the W.K.B. quantization conditions were used in quantum mechanics for many decades it was Keller (Keller 1958 and Keller and Rubinow 1960) who formulated them systematically for systems with many dimensions. These conditions have been reviewed by Percival (1977). They are commonly called E.B.K. quantization conditions since. In our cases :

$$I_r = (n_r + \frac{\alpha}{4} + \frac{b}{2})\,\hbar \qquad (5)$$

$$\ell_c = (\ell + \frac{1}{2})\,\hbar \qquad (6)$$

The factor α counts the number of caustics met by the contour C_r while b is the number of times C_r touches a boundary. The factor $\frac{1}{2}$ put in the angular momentum quantization, the Langer correction, is due (Keller and Rubinow 1960), to $\alpha = 2$ encounters of the angular contour with a conical caustics. These caustics are absent in two dimensions. The actions may also be interpreted as radii of tori on which lie the trajectories (Berry, 1981).

For the potentials considered later we have the values :

. infinite spherical well : $\alpha = 1$, $b = 1$;

. harmonic oscillator, diffuse well : $\alpha = 2$, $b = 0$.

From now on the actions will be divided by $\hbar$.

The semiclassical values of the energy obtained by this method are represented by points standing on the classical energy action-surface. Suppose now that a parameter of the potential, like the radius, is continuously changed.

The energy-action surface will evolve in its three dimensional space and the change of the semiclassical eigenvalues will be explained entirely by this smooth change of the surface. In other words each classical torus which corresponds to a quantum eigenvalue will smoothly evolve and will carry with it the quantum numbers. This is accomplished in the spirit of the Ehrenfest adiabatic invariants. In this way we will show that we can explain every spherical single particle orbit for all nuclei by a continuous change of the radius of the potential. One can easily transform, for example, the 1s state of the lead nucleus into the 1s state of the gold nucleus.

3. Limiting cases of the diffuse potential

1 . The diffuse potential

We will use in this paper the diffuse spherical well introduced by B. Buck and A.A. Pilt (1977) defined as

$$V(r) = - V_o \quad \frac{1 + \text{ch } R/a}{\text{ch } r/a + \text{ch } R/a} \qquad (7)$$

The advantage over the Woods Saxon is that $\frac{dV}{dr} = 0$ for $r = 0$ and the difference is negligible apart from this smoother behaviour. It is this potential that will also be considered in a future publication with an ellipsoïdal deformation.

The actual nuclear field is known to contain in addition to (7) a spin-orbit part and, for protons, a Coulomb repulsion. The Coulomb term could be treated easily as a modification of the central field. But a difficulty arises for the $\vec{\ell} \cdot \vec{s}$ term which has no classical counterpart. It could be overcomed by introducing separately two potentials $\frac{1}{2}\ \ell_c\ V_{so}(r)$ and $-\frac{1}{2}\ (\ell_c + 1)\ V_{so}(r)$ for $j = \ell + 1/2$ and $\ell - 1/2$ respectively. Since our

aim is to work completely in classical physics, this will not be done here, and for simplicity we will treat only the motion of a neutron in the diffuse well Eq (7).

2 . The harmonic oscillator

A nuclear potential is commonly approximated by an harmonic oscillator. Although this potential is a textbook exercise its properties are so important for the following that they need to be briefly reminded (Goldstein 1980). The contour $\{r, p_r(E, \ell_c)\}$ for $\ell_c = 0$ is easily seen to be a half ellipsis, its area divided by 2π is $I_r = E/2\omega$. Since the motion is completely degenerate H is a function of the combination $2 I_r + I_\theta + I_\phi$ (the radial frequency is twice the angular one). Using eq (3) we find the well known result

$$E = (2 I_r + \ell_c)\, \omega \qquad (8)$$

which coincides with the quantum mechanical one if one uses eq (5) and (6). The energy-action surface is a plane, its intersection with $E = c^{te}$ is a straight line the slope of which in the $\{\ell_c, I_r\}$plane is $-\frac{1}{2}$. This slope leads to the well known degeneracies of the quantum harmonic oscillator. The curves $\{ r, p_r(E, \ell_c) \}$ are oval like, the elliptic fixed point corresponds to $\ell_{c\,max} = E/\omega$. The set with $0 \leqslant \ell_c \leqslant \ell_{cmax}$ bound by the half-ellipsis represents all possible radial motions. Fig. 3 shows a plot of I_r versus E for $\ell = 0, 1, 2$, etc...

What oscillator approximate the best the diffuse potential, what is then the domain of validity of this approximation ? These questions are not completely understood. We want to suggest here that the best oscillator is the

one which has its energy action surface nearer from that of the diffuse potential. It is therefore necessary to determine whether this surface can be approximated by a plane and where do the deviations occur and where do they come from.

3 . The infinite spherical well or the spherical billiard

For large R/a our diffuse potential can be reasonably approximated by a spherical square well. The results of a quantum calculation for this well are found in Green et al.(1968) and its semiclassical quantization was studied equally long ago (Keller and Rubinow 1960) in two dimensions. The radial motion is made by coplanar chords between two successive collisions with the boundaries. If R_o denotes the radius of the well, R the shortest distance of the trajectory to the center it is easily found that

$$I_r = \frac{1}{\pi}\sqrt{2mE}\ R_o\left(\sqrt{1-\left(\frac{R}{R_o}\right)^2} - \frac{R}{R_o}\,\mathrm{Ar}\cos\frac{R}{R_o}\right) \qquad (9)$$

$$\ell_c = \sqrt{2m}\,E\ R \qquad (10)$$

which form a parametric representation of the energy-action surface in terms of R, the radius of the spherical caustics. This surface is not a ruled surface like for the harmonic oscillator or the hydrogen atom. (The two cases where Bertrand's theorem apply and where E is a function of $2\,I_r + \ell_c$ or $I_r + \ell_c$).

The curves $\{r, p_r(E, \ell_c)\}$ are simply given by

$$p_r = \sqrt{2\,m\,E}\qquad\sqrt{1-\frac{R^2}{r^2}} \qquad (11)$$

The fixed point of the Poincaré mapping has the maximum radius $R = R_o$, while the contour is a rectangle of sides R and $2\sqrt{2mE}$. The energy spectrum of a

spherical well is known to contain R_0 just as a scaling factor. On the other hand the section of the energy action surface by a plane $E = c^{te}$ is a curve which can be simply scaled according to the energy. Let us introduce reduced actions $\tilde{I}_r$, x by

$$\tilde{I}_r = \pi I_r / \sqrt{2m E}\, R_0 \qquad x = \frac{\ell_c}{\sqrt{2m E}\, R_0} = \frac{R}{R_0} \tag{12}$$

then

$$\tilde{I}_r = \sqrt{1 - x^2} - x \operatorname{Ar} \cos x \tag{13}$$

The comparison of the semiclassical energies with the solutions of the Helmholtz equation was already performed (Keller and Rubinow 1960) in two dimensions. We will do it here with the help of the the universal function $\tilde{I}_r(x)$ which can be used both for two and three dimensions. The solutions of the wave equations (cylindrical or spherical Bessel functions) lead us to sets of points :

$$\left\{ \frac{\ell + 1/2}{(k R_0)_3}\ ,\ \frac{n_r + 1/2}{\pi (k R_0)_3} \right\} \quad \text{in three dimensions,}$$

$$\left\{ \frac{\ell}{(k R_0)_2}\ ,\ \frac{n_r + 1/2}{\pi (k R_0)_2} \right\} \text{ in two dimensions}$$

which can be plotted on the $\{x, \tilde{I}\}$ plane. It is seen in Fig. 4 that the very good agreement between the semiclassical method and the wave mechanics is common to 2 and 3 dimensions. Moreover the energy-action surface is the same for both cases. The lattices of quantization are displaced by a translation of 1/2 unitparallel to the ℓ_c axis. (The effect of the supplementary caustic (Keller and Rubinow 1960)).

The curvature of the energy action surface visible in Fig. 5 originates from that of the universal function $\tilde{I}_r(x)$. It has consequences on the ordering of the single particle levels. Indeed the slope of $I_r(x)$ takes its lower

value - 1/2 for $x = 0$. The curve is then always concave upwards and the slope increases to zero. From this rule it is deduced that the energy of the terms of a harmonic oscillator multiplet (which need the slope - 1/2 to be degenerate) are not any more the same and that the higher the ℓ the lower the energy. In the example of the shell N = 4 the energies of the subshells are ordered as

$$E_{1g} < E_{2d} < E_{3s} \tag{14}$$

The splitting of the harmonic oscillator major shells is well known to be produced by a finite size effect of the potential. The primitive manifestation of this effect lies in the curvature of the classical energy action surface. Another of its manifestation is seen on Fig. 6.

Again the comparison of the energy action surface of the diffuse well to the present one will help us to determine the situations under which its spectrum is best represented by that of the spherical well.

4 . Semiclassical quantization of the diffuse well

In the following we want to describe the shape of the energy action surface of the Buck-Pilt potential for a very broad range of nuclei : $16 \leqslant A \leqslant 208$. The evolution with A of the semiclassical energies will then be connected to the changes of this surface in the spirit developed at the end of § 2.2. The semiclassical values will then be compared to the eigenvalues of the Schrödinger equation.

1 . Extreme values of A

We describe first the surface for the two extreme cases

$$A = 16 \qquad \frac{R}{a} = 4.898 \tag{15}$$

$$A = 208 \qquad \frac{R}{a} = 11.517 \tag{16}$$

The depth parameter V_0 will take the value 52 MeV. We will use sometimes $\eta = 1 - \frac{|E|}{V_0}$ instead of E. Figures 7 and 8 represent the curves $\{r, p_r(\bar{E},0)\}$ i.e. the contour of the Poincaré sections for several values of E. For A = 16 the contour is mostly an half-ellipsis for low η. However if $\eta \to 1$ an inflexion point occurs and allows p_r to be a slower decreasing function of r for large r. This surface effect corresponds to the smooth slowing down of the particle when r is large. It leads to an enlargement of the radial phase space. Note indeed that $r \to \infty$ when $p_r \to 0$ if $\eta \to 1$. It produces a comparatively larger slope of the action for $\eta \to 1$ for the small ℓ. On Fig. 9 the radial action of the $\ell_c = 0$ trajectories is represented by a dotted curve which is clearly non linear near $\eta = 1$. This effect is seen for $\ell_c = 1/2$ (s states) to the same extent, it is visible also to a less degree for $\ell_c = 3/2$ and $5/2$. Consequently an eigenstate with these conditions (small ℓ, large η) is quantized for a smaller energy than expected for a potential for which the linearity is either exact (harmonic oscillator Fig. 3 or at least a good approximation (the billiard Fig. 6). This effect is susceptible to change significantly the ordering of the single particle levels in the vicinity of the upper part of the spectrum. It produces a higher level density in this region.

In the case of A = 208 (Fig. 8) the contour is mostly a rectangle, like in the billiard, but the corners are rounded since there is no specular reflexion. The inflexion of p_r is still present to a certain extent for large η.

The representation of the energy action surface which is done through Figures 7 to 12 help to understand many facts.

a) case A = 16

The surface is almost a ruled surface everywhere. At small and medium energies it is nearly planar. The major difference with the harmonic oscillator is the surface effect which is visible in the two sections. Note for example on Fig. 11 that the upper curve is not parallel to the others.

When it comes to the semiclassical energies ($E_{s.c.}$ in Table 1) the states 1s, 1p, 2s and 1d are the only bound states and we have the inversion 2s-1d coming from the surface effect.

The quantization conditions being not fulfilled for $\eta > 1$, thus, there is no resonance for any partial wave.

b) case A = 208

As expected the energy action surface is nearer from that of a finite spherical well. Many partial waves have bound states. The curvature of the surface, when shown in the I_r vs. ℓ representation (Fig. 12) has the same sign and qualitatively the same magnitude as the curvature of the billiard seen on Fig. 5.

The order of the energies of the different partial waves and the splitting of the harmonic oscillator multiplets can be seen in Table 2. The curvature produces the splitting in the same direction as in the billiard, i.e. the order described by (14).

The nonlinearity of I_r versus η (Fig. 10) is the highest for the s states. It is clearly responsible from anharmonicities in the spectrum specially for $\eta \sim 0$ or for $\eta \sim 1$. This effect decreases with ℓ. Except for the region of values of η where they end up in the continuum (through the surface effect) the highest ℓ behave in a rather harmonic manner.

Since the surface has a large part at $\eta > 1$ many partial waves, especially the very high ones $\ell = 5,7,8,9$ have resonances at this value of V_0.

The outline of the energy action surface for A = 16 is of great help to understand the connection of the diffuse nuclear potential to the harmonic oscillator for light nuclei, to estimate the most convenient frequency and the extent of the harmonic oscillator approximation. The slopes of I_r versus E shown in Fig. 9 are approximately constant for most values of E and ℓ_c. The slope is $\frac{dI_r}{dE} = \frac{1}{\omega_r}$ where ω_r is the radial frequency at the energy E. Thus it is natural to assign to the equivalent harmonic oscillator a frequency ω equal to $\frac{1}{2}\omega_r$ where ω_r is the natural radial frequency of the particle (Eq. 9) in the region where it is weakly dependent upon the energy. This frequency is definitely not the same as the frequency defined by the curvature of V(r) at r = 0 , i.e.

$$\omega_o^2 = \frac{1}{m} \left.\frac{\partial^2 V}{\partial r^2}\right|_{r=0} = \frac{V_o}{ma^2} \frac{1}{(1+ch\ R/a)} \qquad (17)$$

For A = 16 the mean slope of the dotted line ($\ell_c = 0$) gives -- $\frac{1}{2}\hbar\omega_r \simeq 15.72$ MeV while eq. (17) leads to $\hbar\omega_o = 8.66$ MeV.

In the case of A = 208 we have shown that the energy action surface is more similar to that of a billiard. If however the slope of the $\ell_c = 0$ orbits are calculated using only the linear part (i.e. near the 3s state) it is found that $\frac{1}{2}\hbar\omega_r \simeq 7.78$ MeV. On the other hand $\hbar\omega_o$ takes the absurd value 0.32 MeV ! In this nucleus we have remarked earlier the almost linear slope of I_r for the high ℓ . An average frequency $\bar{\omega}_r^{\ell}$ can be obtained as well for energy ℓ which is weakly dependent upon ℓ .

The values obtained for $\frac{1}{2}\hbar\omega_r$ are in good agreement with the commonly used value $40\ A^{-1/3}$ MeV.

2 . Variation of the semiclassical energies with A

In order to avoid the repetition of the preceding work for each nucleus we have found useful to develop a technique which will help us to follow each energy level individually with A with a sufficient accuracy. This technique is inspired from the Ehrenfest adiabatic invariants.

a) Theory

Suppose that the radius R is given some increase δR corresponding to an increase δA of the number of particles. At a fixed r and given ℓ_c we have then

$$\delta E = \frac{p_r \ \delta p_r}{m} + \frac{\partial V}{\partial A} \ \delta A \qquad (18)$$

but if we impose I_r to be invariant to the second order

$$\delta I_r \simeq \oint_{C_r} \delta p_r \ dr = 0 \qquad (19)$$

After integrating (18) on $_r$, δE is obtained as

$$\delta E = \left[\oint_{C_r} \frac{m}{p_r} \frac{\partial V}{\partial A} \ dr \Big/ \oint_{C_r} \frac{m}{p_r} \ dr \right] \delta A \qquad (20)$$

The migration of the trajectory corresponding to A, I_r, ℓ_c at the energy E to that corresponding to A + δA, I_r, ℓ_c and E + δE is performed by adding to p_r the quantity $\delta p_r(r)$ of (18).

Formula (20) is derived by Landau-Lifshitz (1972) in the frame of the adiabatic invariant theory. It is possible then to draw the curve E(A) for given n_r and ℓ on any interval of values of A, say from A = 208 to A = 16, by dividing this interval into small steps $\delta A = -1$ (or in order to get a better precision $\delta A = -0.2$) and by calculating for each δA

the increase δE and the new contour C_r which will be used at the next step. An orbital like a 1s state for example can be followed with A. Since $\partial V / \partial A$ keeps a constant sign we are able to understand why the single particle levels have a uniform decreasing slope when A is increased. It is also possible to say that the energy action surface is lowered down along the energy axis when A increases.

Although the formula (20) is derived in the field of the adiabatic invariants theory it should be pointed that no time dependence is introduced at any place. Therefore the only approximation done is to use C_r in (19) and not the new contour and to calculate δE with finite increment. The radial action is thus approximately conserved. We will see that the error introduced is small in any case (see Table 1).

b) Results

By using the preceding method it is now possible to calculate $E(\lambda_c, I_r)$ as a function of A for any orbit which fulfills the quantization conditions Eqs (5) and (6). The result presented in Fig. 13 shows the energy levels obtained by this procedure with a step $\delta A = -1$ the initial nucleus being A = 208. The labels of the energy levels can be obtained by following each level and by inspecting Table 2 for A = 208.

The evolution of the levels of Fig. (12) can be now explained in terms of the effects already discussed.

1) The uniform sloping down of each energy level with A is due to the negative sign of δE in eq. (20)

2) The spitting of the terms of each harmonic oscillator multiplet is that of the billiard for deep and moderately deep bound states.

3) The crossings of energy levels are produced only in the upper part of the spectrum. There the states with smaller ℓ tend to be at a lower energy. This can be interpreted in every case as a manifestation of the surface effect discussed for A = 16. An enlargement of the level scheme is shown on Fig. (14) for the 3s-2d-1g orbits. The crossings are also present in the exact eigenvalues. However since the semiclassical energies are too high by about 1 MeV in this region, the values of A for which they occur are wrong by 2 to 4 units.

4) Families of resonant states are produced. The family with $n_r = 1$ end up at the higher energy, then comes the $n_r = 2$ family etc...

The outline of the level spectrum of Fig. 13 has been obtained a long time ago by Green et al (1968) by solving the Schrödinger equation with slightly different potentials. We have explained above the details of this figure almost entirely by classical mechanics.

3 . *Comparison with the quantum results*

We have compared the semiclassical energies E_{sc} to results obtained by solving numerically the Schrödinger equation. Two methods were used. The first is the diagonalization of the hamiltonian in a troncated basis which contains 11 oscillator shells for all the values of A. The results are denoted by E_Q^T The second method is an integration in the configuration space using Numerov and Cooley's method (Numerov 1933 and Cooley 1961) based on a recurrence relation valid up to the sixth order of the integration step . The results of which are denoted as E_Q^N.

The quantum resonances are defined as in Gamow's theory of the alpha decay. In that case this definition is the nearest from the classical one.

Thus when the energy becomes positive the effective potential is kept constant from the point where it takes its maximum value up to infinity (instead of falling to zero). In this approximation the quantum resonances are calculated as bound states. However this sudden change in the potential produces a discontinuity on the energy when it passes throughout zero. This effect can be seen on Fig. 14 which shows the crossing of the N = 4 quantum levels. No attempt has been made to calculate the resonance energy in a more exact way.

For each given partial wave, the semiclassical bound states and the resonances are all obtained when the energy is smaller than the maximum value of the effective potential (provided this maximum do exist).

The energies E_{sc} are found by solving eq.(5)-(6) until I_r takes the prescribed value up to 10^{-6}.

Table 1 contains in addition to E_{sc} the values obtained by using the adiabatic invariants method which allowed us to write Eq. 20. At each step δA a slight error is introduced both on I_r and δE, the starting values being taken from A = 208 (Table 2).This error is not found to change significantly the results for ^{16}O which means that Fig. 13 and 14 are correct for all intermediate nuclei.

The semiclassical energies are generally within less than 1 MeV apart from the more exact value E_Q^N. The difference between E_Q^N and E_{sc} does not change much with A (intermediate values of E_Q^N have also been calculated some of which are given in Table 3). This difference is shown in more detail in Fig. 14 for the N = 4 shell between A = 30 and A = 50 for which three interesting crossings occur. Due to this rather constant error the crossings are not produced at the right place but 2 to 4 units of A apart from the quantum mechanical ones. This behaviour is typical and can be applied to all the crossings which occur on Fig. 13.

The difference between E_Q^T and E_Q^N is not very significant for deep bound states and also for A = 16. For the slightly bound states of A = 208 the diagonalization in a truncated basis provides results of the same quality as E_{sc}.

The comparison between E_{sc} and E_Q^N has thus not the same quality for the diffuse well as that shown for the infinite well on Fig. 4 and in Keller and Rubinow (1960). This means that the correct eigenvalues are located even farther away from the classical energy action surface for the diffuse potential.

A possible approach of the difference $E_Q^N - E_{sc}$ could be the calculation of the second and higher order WKB corrections. In the case of Lennard Jones potential (Krieger and Rosenzweig, 1964 and Kesarwani and Varshni 1978 and 1980) these corrections are found to improve in a spectacular manner the simple WKB energies. If the action is measured in units of h by

$$\xi = \frac{\pi \sqrt{2m V_0}\, R}{h}$$ as in Kesarwani and Varshni (1978,1980)

we find that $\xi = 1.99$ for A = 16 and 4.69 for A = 208 while in Kersarwani and Varshni (1978,1980) ξ takes the values 5,12,25 and 50. We can compare our potential, in the best case, to the value $\xi = 5$ of the Lennard Jones potential. The very detailed analysis performed in Kesarwani and Varshni (1978,1980) up to the sixth power in $\hbar$ makes us confident that the differences $E_Q^N - E_{sc}$ can be handled in that way.

5 . Conclusion.

The specific property of integrable systems is the existence of a surface energy action on which are concentrated all the information on the bound trajectories. In very few cases like the harmonic oscillator or the hydrogen atom the relation between the energy and the actions is analytical. In other cases, like the diffuse potential studied in this paper, this relation can be established only with the help of a numerical calculation. This surface is the natural mathematical object by which the connection can be drawn between classical mechanics and quantum mechanics through the semiclassical method EBK. In particular we have shown that its geometrical properties : curvature, slope, etc... are the simplest ingredients through which an understanding of the semiclassical spectrum is obtained. Although the comparison with the exact quantum mechanical spectrum reveals significant numerical differences, the properties of the single particle spectrum and their evolution throughout the set of nuclei are qualitatively understood by the properties of the classical surface and by its changes with the number of particles.

In a future publication we will try to sketch the energy action surface as far as possible in the deformed, non integrable, cases. Since our preliminary study (Carbonell 1983) has shown that the threshold of occurrence of chaotic trajectories leaves large parts of regions in the parameter space where the trajectories lie on K.A.M. tori this program can be fulfilled to a certain extent. The properties of the single particle spectrum : splitting, anharmonicity, crossings etc... can then be tentatively connected to the classical surface.

Figure captions

Figure 1 - The classical energy-action surface for light (^{16}O), medium (^{90}Zr) and heavy nuclei (^{208}Pb) for the Buck-Pilt potential with V_0 = 52 MeV. The surfaces are viewed from the same angle and are represented with the same scale. In addition actions are in units of h. With this angle of sight it clearly appears that the surface is mostly planar for ^{16}O and gets a curvature when A is increased. The surfaces are bounded by the linear trajectory curve ($\ell_c = 0$), the circular trajectory curve ($I_r = 0$) and the asymptotic aperiodic trajectory which also limits the unbound states. The changes of the surface with A produces the semiclassical level scheme of Fig. 13.

Figure 2 - The radial phase space $\{r,p_r\}$ of the diffuse potential at two values of the energy $\eta = 0.5$ and $\eta = 0.99$ for A = 16, η is defined as $1 + E / V_0$. Note the increase of the size of phase space for the more peripheral (small ℓ_c) trajectories at $\eta = 0.99$. This surface effect explains the order 2s-1d (see Fig. 9). For $\eta = 0.5$ the picture is very similar to that found for the harmonic oscillator.

Figure 3 - Sketch of the radial action for a harmonic oscillator. Each line corresponds to a different ℓ_c. The energy unit is arbitrary

Figure 4 - The reduced action curve for the spherical billiard. Points shown represent the wave mechanical values in 2 and 3 dimensions. For convenience 16 well separated eigenvalues are represented.

Figure 5 - Intersection of the energy action surface with plans $E = c\frac{t}{=}$ for an infinite spherical billiard. Note the curvature of the surface. Values $E = c\frac{t}{=}$ have been taken. The lattice shown represents the allowed wave mechanical values.

Figure 6 - Radial actions of the billiard as a function of E. These plots provide directly the semiclassical energies. The splitting of the N = 4 harmonic oscillator shell is directly seen and the rule (14) is here justified.

Figure 7 - Contour of the $\{r,p_r\}$ plot at various energies for the diffuse potential for A = 16. At the lower η the contour is almost a half ellipsis. A surface effect occurs at the higher η . The size of $\hbar$ is indicated by the dashed surface.

Figure 8 - Same as in Fig. 6 but for A = 208. The contour is almost rectangular like for the spherical billiard. The surface effect is also seen.

Figure 9 - Radial action v.s. energy η is shown for the diffuse potential and A = 16. The dotted line corresponds to $\ell_c = 0$ trajectories (the contours shown in Fig. 7). Only s-p and d states are bound. The difference with Fig. 3 lies in the change of slope of I_r at the higher η (surface effect). Without this surface effect the 2 s states would be above the 1d state as represented on the figure.

Figure 10 - Same as Fig. 8 for A = 208. Note the great number of bound states. The rule (14) is obtained for the N = 4 multiplet like in Fig. 5.

Figure 11 - Sections of the energy action surface for A = 16 for the diffuse potential at η = 0.2, 0.4, 0.6, 0.8, 1 and 1,2. This surface is

seen to approach very nearly a ruled surface. The surface effect introduces a loss of parallelism of the curve $\eta = 1$ with the others. The quantum mechanical values of the actions are shown by a lattice.

Figure 12 - Same as Fig. 10 for A = 208 up to $\eta = 1.8$. The surface is very similar to that represented on Fig. 4 for an infinite billiard.

Figure 13 - Semiclassical single particle energies and resonances of a neutron in the nuclei with $16 \leqslant A \leqslant 208$. Equations (5) and (6) have been solved for A = 208 then each torus is followed by use of eq. (20) and finally A = 16 is obtained. The label of each single particle state can be determined by inspecting Table 1 and 2.

Figure 14 - An enlargement of the encircled part of Fig. 13 is presented. The semiclassical energies can be compared to the exact quantum mechanical eigenvalues. All the crossings predicted by considering the energy action surface are seen to be produced in quantum mechanics a few units of A away.

	E_{sc}	$\delta A = -0.2$	$\delta A = -1.0$	E_Q^N	E_Q^T
1s	-32.4 15	-32.550	-32.863	-32.5881	-32.5907
1p	-17.2477	-17.352	-17.763	-18.0238	-18.0252
2s	- 3.6362	- 3.687	- 3.899	- 4.4257	-4.3325
1d	- 2.5237	- 2.614	- 2.979	- 3.7912	-3.7610

Table 1

	E_{sc}	E_Q^N	E_Q^T
1s	-48.2122	-47.8033	-47.7984
1p	-43.9895	-43.6883	-43.6904
1d	-38.8896	-38.7154	-38.7088
2s	-36.9177	-36.8649	-36.8524
1f	-33.0154	-32.9863	-32.9680
2p	-30.0339	-30.1416	-30.1080
1g	-26.4505	-26.5825	-26.5616
2d	-22.6835	-22.9483	-22.9008
3s	-21.3253	-21.6285	-21.5696
1h	-19.2696	-19.5776	-19.3700
2f	-14.9906	-15.4110	-15.0696
3p	-13.1420	-13.5817	-13.1820
1i	-11.5463	-12.0459	-11.8716
2g	-7.1228	- 7.6970	- 7.3892
3d	-5.2936	- 5.8421	- 5.4600
4s	-4.7662	- 5.2739	- 4.8516
1j	-3.3598	- 4.0708	- 3.5100
Resonances			
2h	+ 0.6511	-0.925	
3f	+ 1.3262	+ 0.9735	
1k	+ 5.1939	+ 4.3916	
2i	+ 7.6081	+ 7.6291	
1l	+13.9775	+13.2494	
1m	+22.7132	+22.6477	

Table 2

	$E_Q^N - E_{s.c.}$			
A	1s	3s	1d	1g
16	-0.1186		- 1.2675	
28	+0.1559		- 0.8799	
40	+0.2780		- 0.6118	
64	+0.3780	-0.5600	- 0.2944	-0.9952
90	+0.4134	-0.5978	- 0.1089	-0.6847
132	+0.4243	-0.4853	+ 0.0493	-0.3936
160	+0.4209	-0.4084	+ 0.1099	-0.2719
208	+0.4089	-0.3032	+ 0.1742	-0.1320

Table 3

References

Balian R. and Bloch C. 1970 Ann. Phys. 60 401-47

1972 Ann. Phys. 69 76-160

1974 Ann. Phys. 85 514-45

Berry V. 1981 Les Houches (Amsterdam : North-Holland) 171-271

Berry V. 1981 Eur. J. Phys. 91-102

Berry V. 1981 Les Houches (Amsterdam : North-Holland) 171-271

Bohr A. and Mottelson B. 1975 Nuclear Structure Vol. II 579-98 (Reading, Mass : Benjamin)

Bountis T.C. 1981 Physica 3D 577-89

Buck B. and Pilt A.A. 1977 Nucl. Phys. A 280 133-160

Carbonell J. 1983 Thèse de 3ème cycle Université de Grenoble

Carbonell J. and Arvieu R. 1983 Nuclear Fluid Dynamics (ICTP : Trieste) 141-44

Cooley J.W. 1961 Math. Comp. 363-74

Einstein A. 1917 Ver. Dent. Phys. Ges. 19 82-92

Goldstein G. 1980 Classical Mechanics (Reading, Mass. : Addison Wesley)

Green A.E.S., Sawada T. and Saxon D. 1968. The Nuclear Independent particle model (New-York, London : Academic Press)

Gutzwiller M. 1967 J. Math. Phys. 8 1979-2000

1971 J. Math. Phys. 12 343-58

Henon M. 1981 Les Houches (Amsterdam : North-Holland) 53-170

Henon M. and Heiles C. 1964 Astron. J. 73-79

Gutzwiller M. 1982 Physica 5D 183-207

Keller J.B. 1958 Ann. Phys. 4 180-88

Keller J.B. and Rubinow S.I. 1960 Ann. Phys. 9 24-75

Kesarwani R.N. and Varshni Y.P. 1978 Can. J. Phys. 56 1488-93

1980 Can. J. Phys. 58 363-69

Krieger J.B. and Rosenzweig C. 1964 Phys. Rev. 164 171-73

Landau L. and Lifshitz E. 1972 Mécanique (Mir : Moscou)

Noid D.W., Koszykowski M.L. and Marcus R.L. 1981 Ann. Rev. Phys. Chem. 32 267-309 and references contained therein

Numerov B. 1983 Publ. Obs. Cent. Astr. Russ. 2 188

Percival I. 1977 Adv. Chem. Phys. 36 1-61

Reinhardt W. 1982 J. Phys. Chem. 86 2158-65

Robnik M. 1981 J. Phys. A 14 3195-216

Schuck P. 1983 Lectures Notes at the Alcabideche School on Density Functional Methods in Physics and references contained therein. To be published by NATO Advanced Study Institutes Programm.

Strutinsky V.M. 1967 Nucl. Phys. A 95 420-42

1968 Nucl. Phys. A 122 1-33

1974 Nucleonica 20 679-715

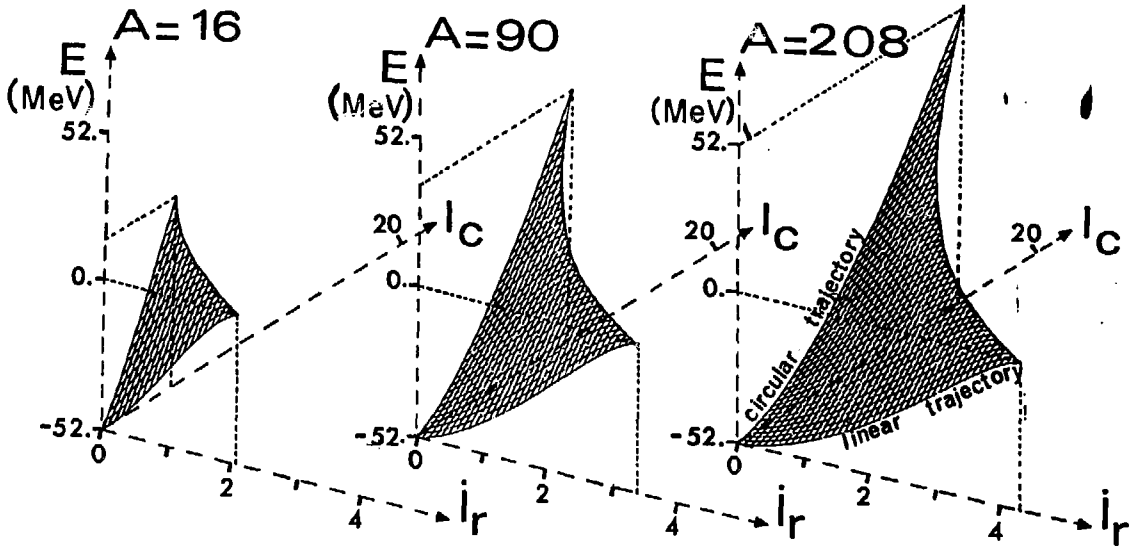
A=16
E
(MeV)
52.
0.
-52.
0
2
4
i_r
A=90
E
(MeV)
52.
20
I_c
0.
-52.
0
2
4
i_r
A=208
E
(MeV)
52.
20
I_c
0.
-52.
0
2
4
i_r
20
I_c
circular trajectory
linear trajectory

Fig. 1

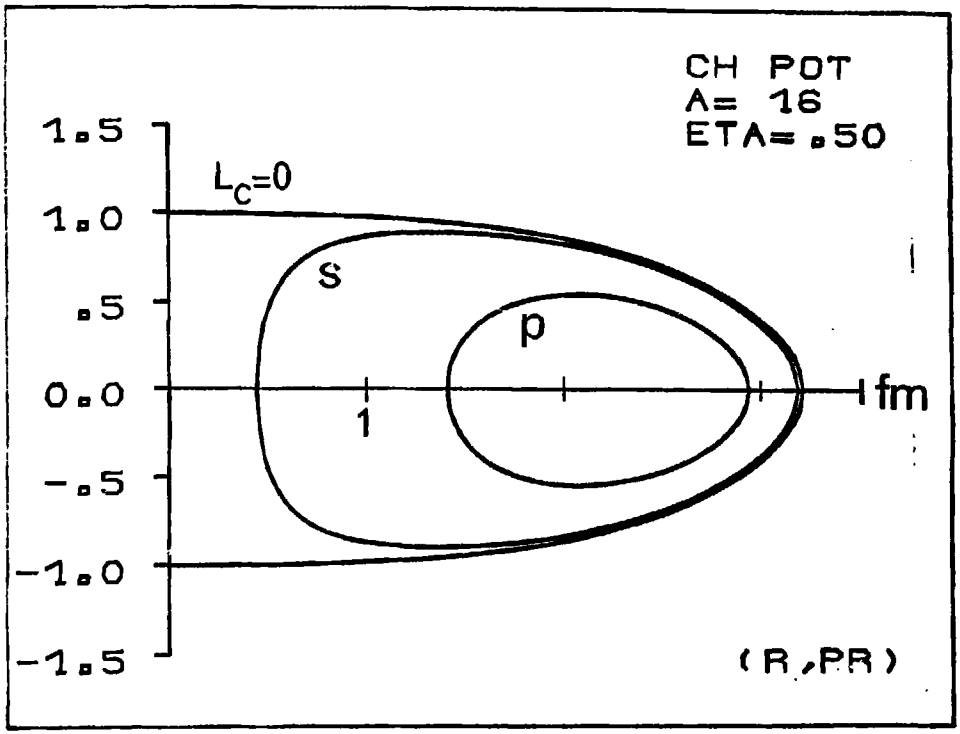

Fig. 2a

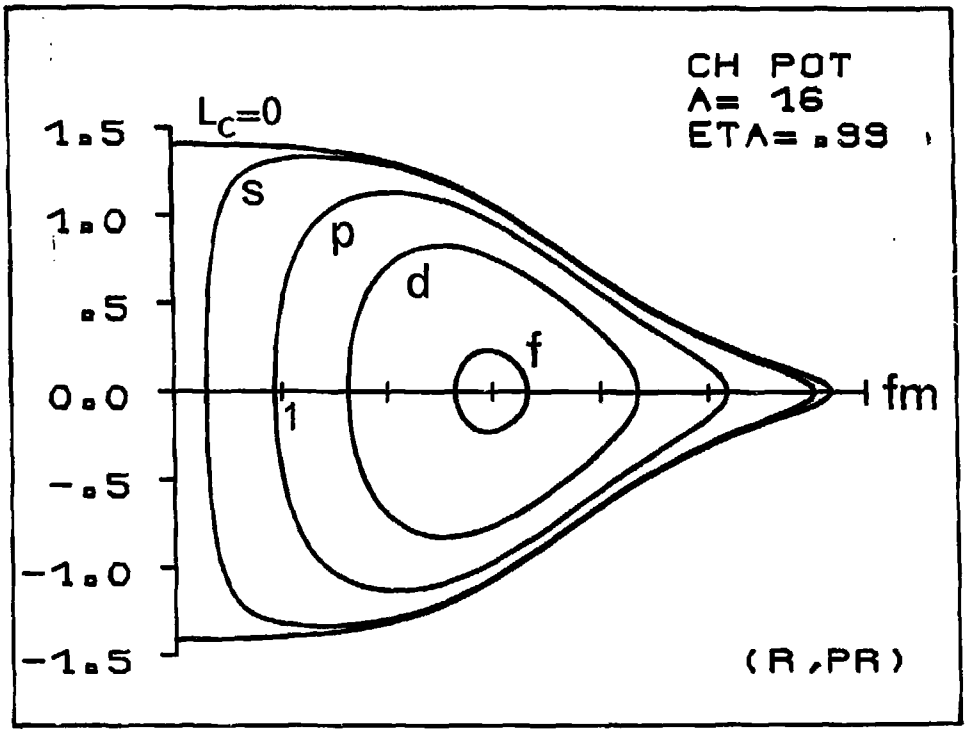

Fig. 2b

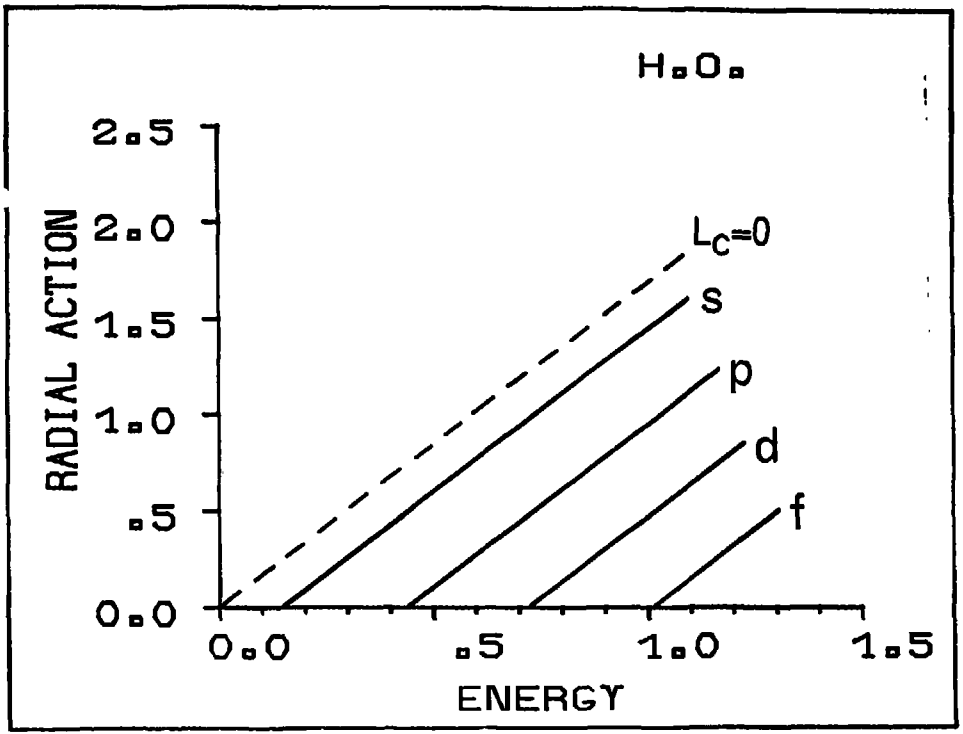

Fig. 3

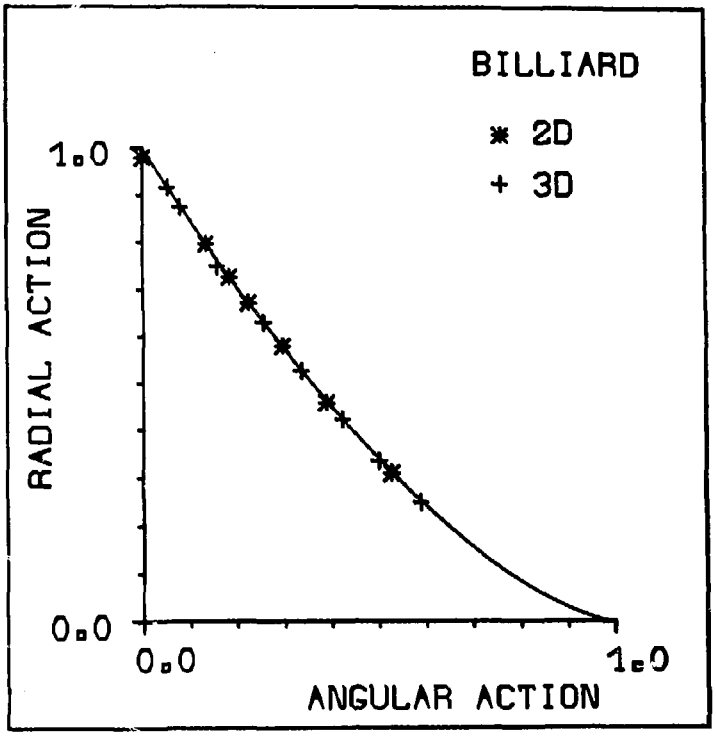

Fig. 4

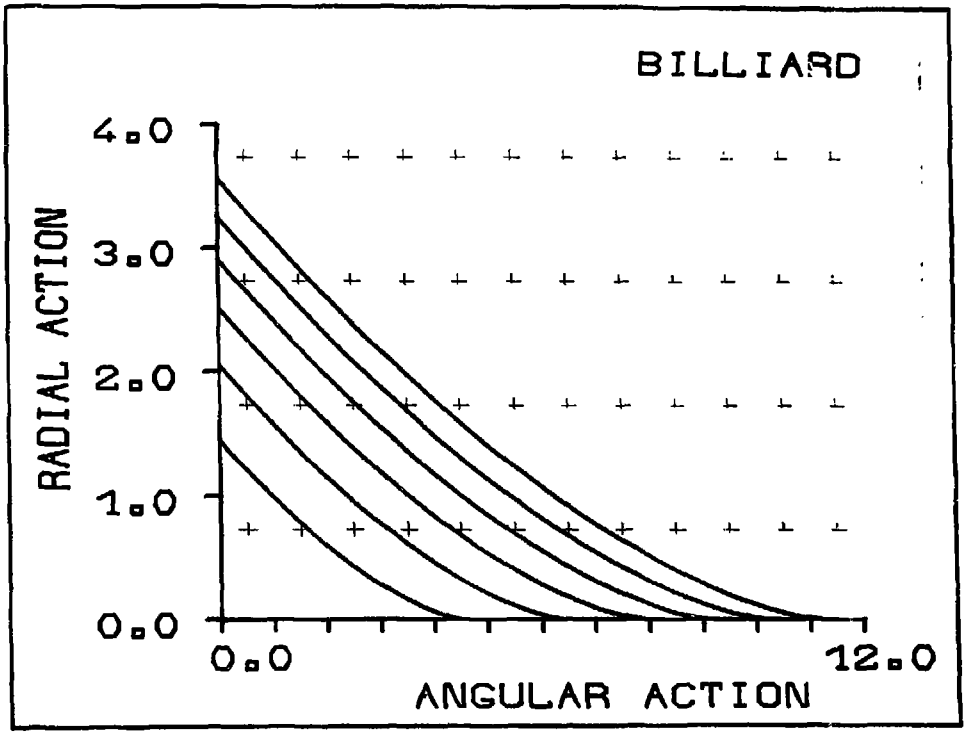

Fig. 5

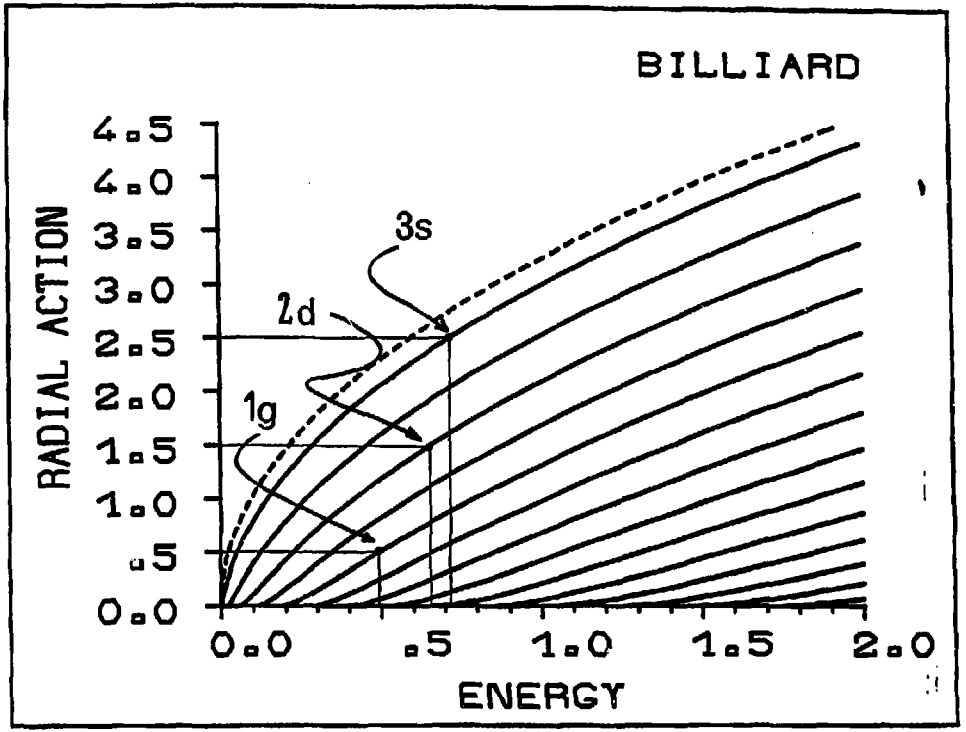
BILLIARD
RADIAL ACTION
4.5
4.0
3.5
3.0
2.5
2.0
1.5
1.0
.5
0.0
3s
2d
1g
0.0
.5
1.0
1.5
2.0
ENERGY

Fig. 6

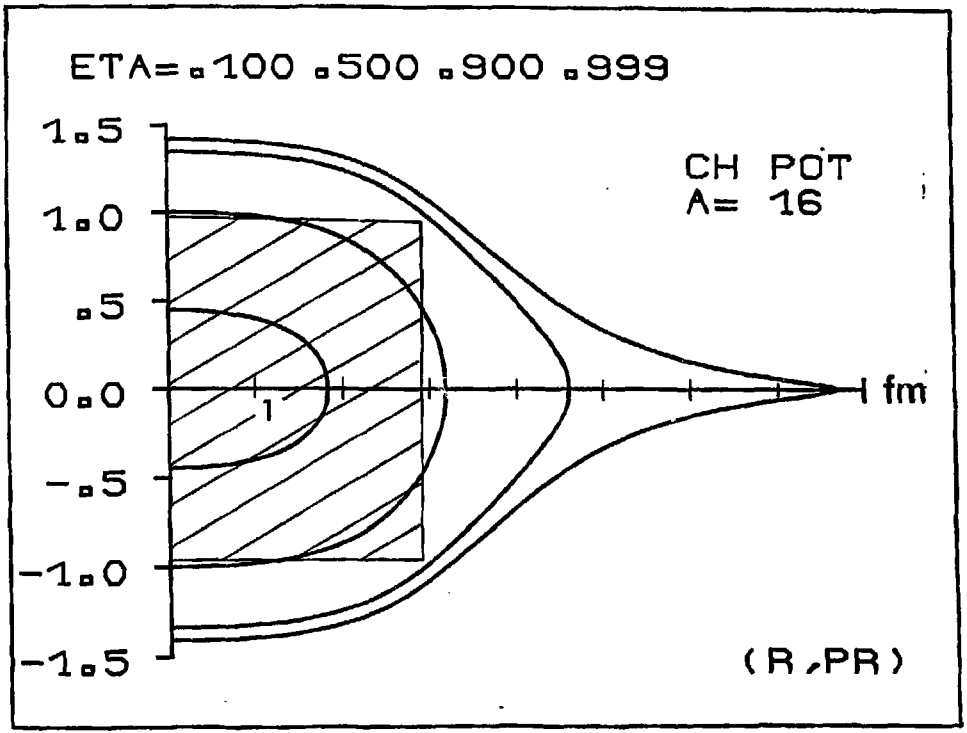

Fig. 7

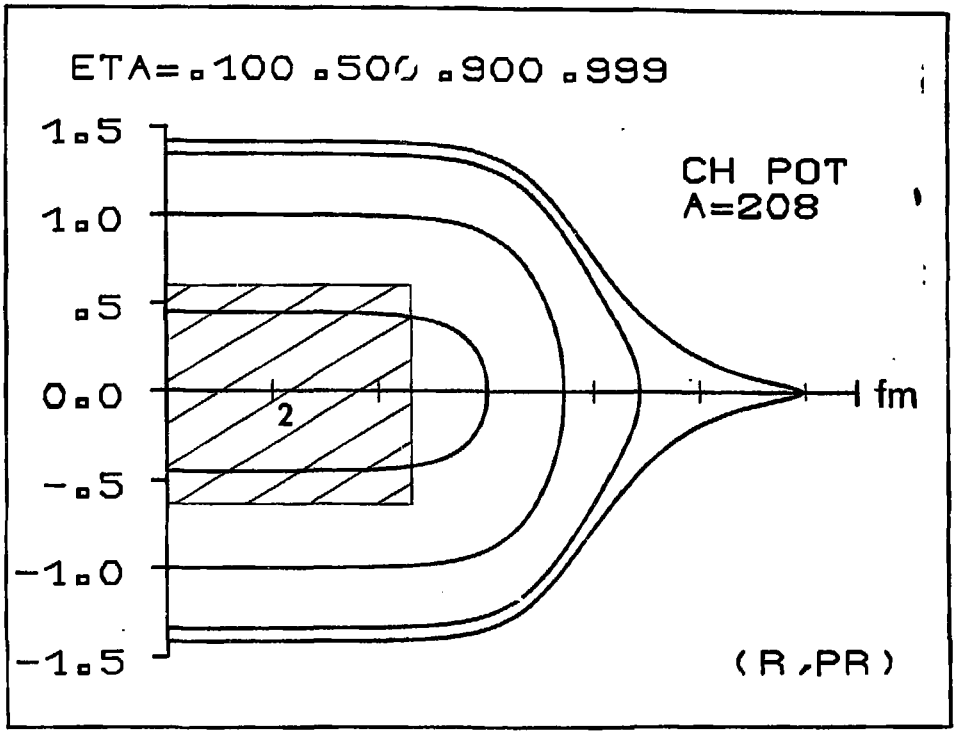

Fig. 8

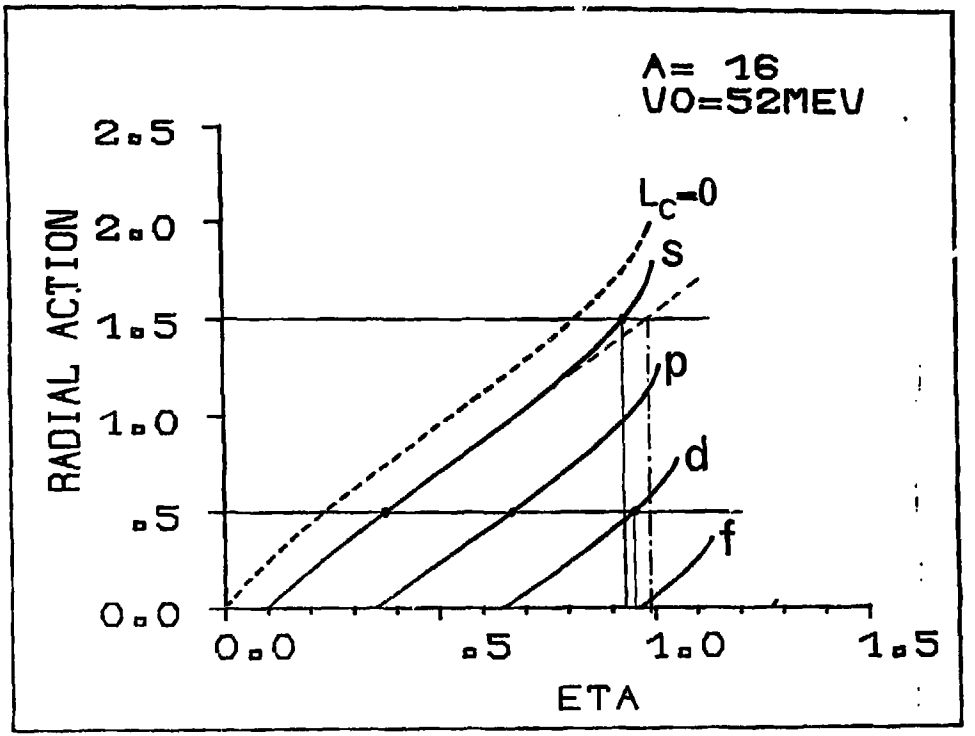
A= 16
VO=52MEV
2.5
2.0
1.5
1.0
.5
0.0
RADIAL ACTION
L_c=0
s
p
d
f
0.0
.5
1.0
1.5
ETA

Fig. 9

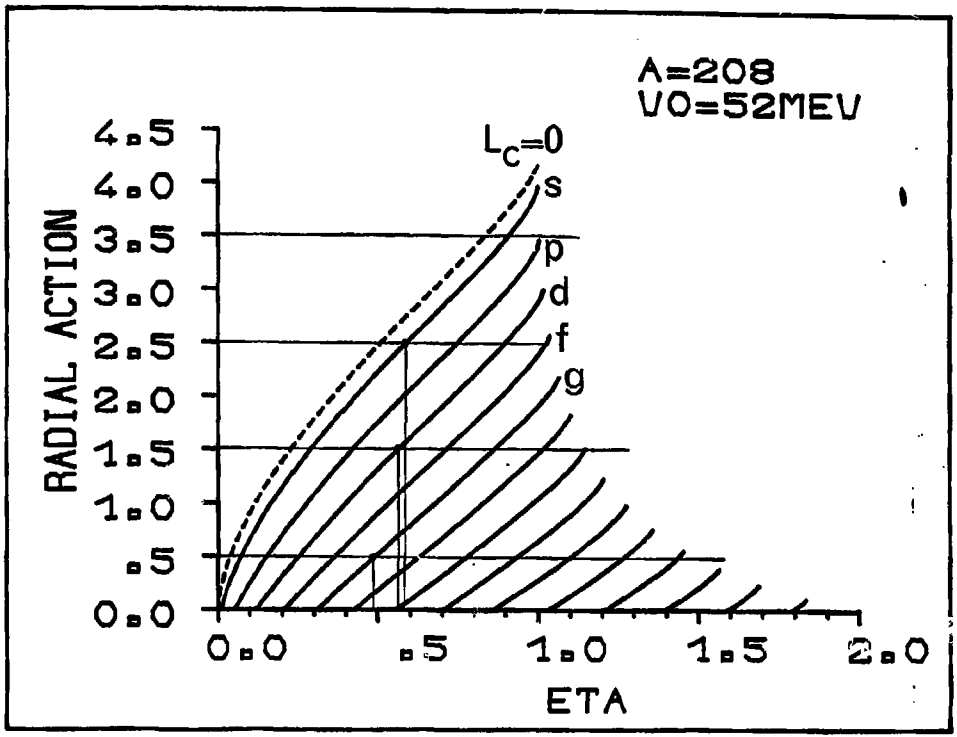
A=208
V0=52MEV
L_c=0
s
p
d
f
g
RADIAL ACTION
4.5
4.0
3.5
3.0
2.5
2.0
1.5
1.0
.5
0.0
0.0
.5
1.0
1.5
2.0
ETA

Fig. 10

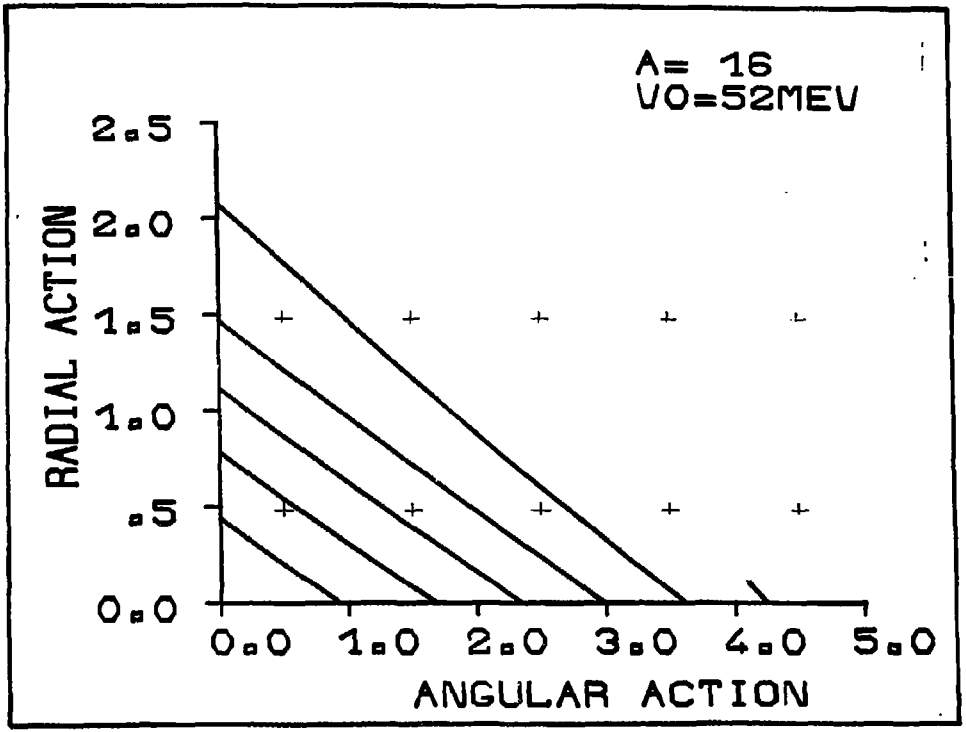
A= 16
VO=52MEV
RADIAL ACTION
2.5
2.0
1.5
1.0
.5
0.0
0.0
1.0
2.0
3.0
4.0
5.0
ANGULAR ACTION

Fig. 11

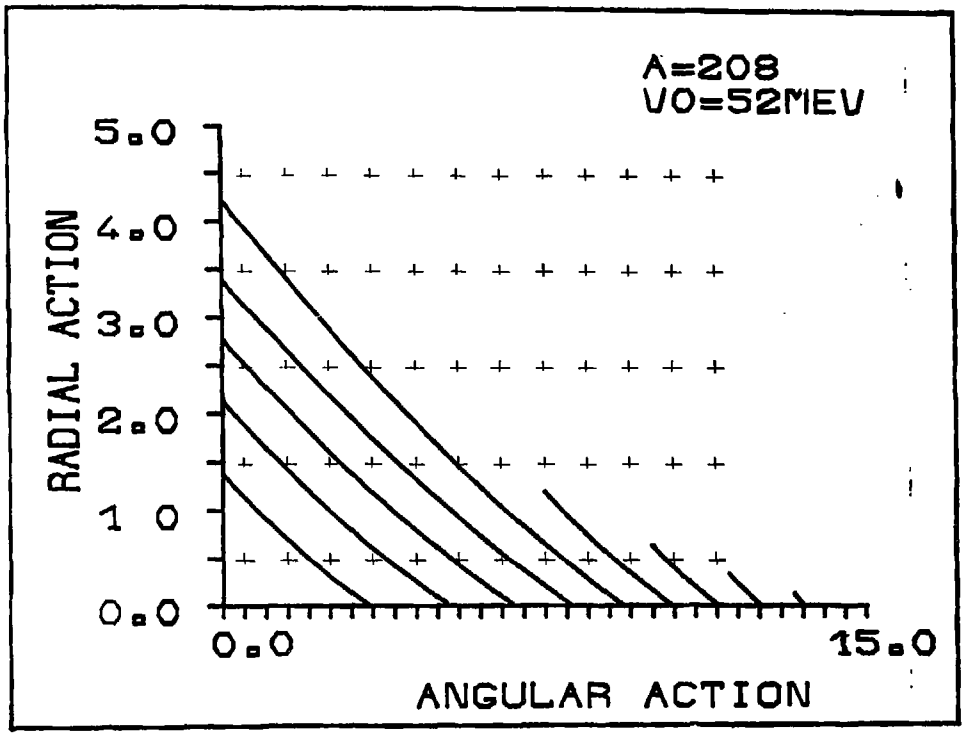
A=208
V0=52MEV
5.0
4.0
3.0
2.0
1 0
0.0
RADIAL ACTION
0.0
15.0
ANGULAR ACTION

Fig. 12

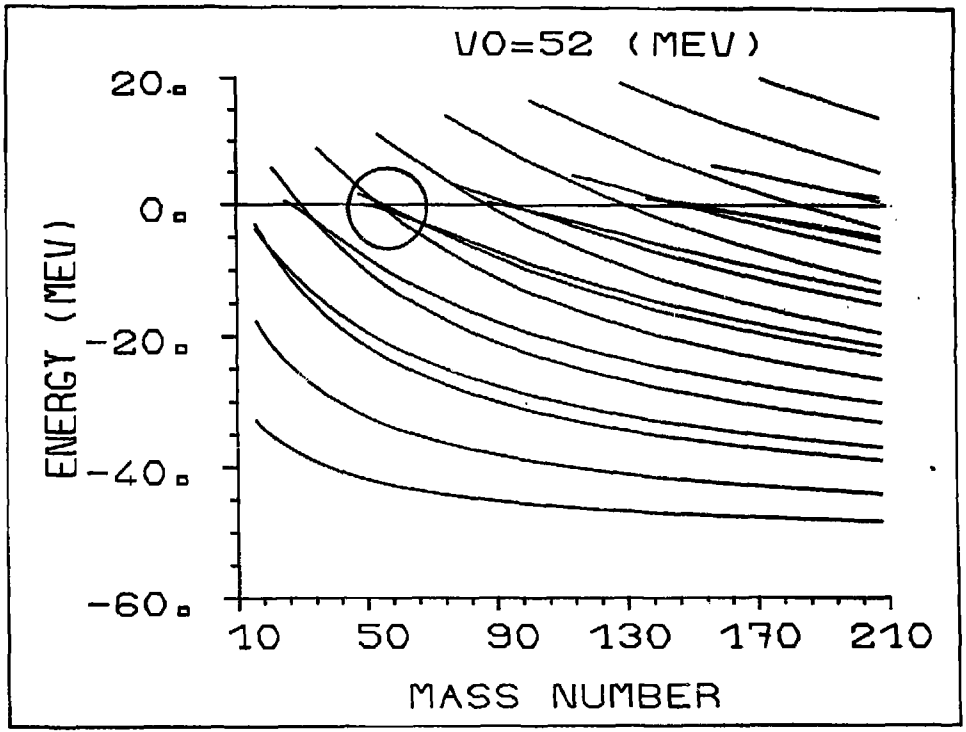
V0=52 (MEV)
20.
0.
-20.
-40.
-60.
ENERGY (MEV)
10
50
90
130
170
210
MASS NUMBER

Fig. 13

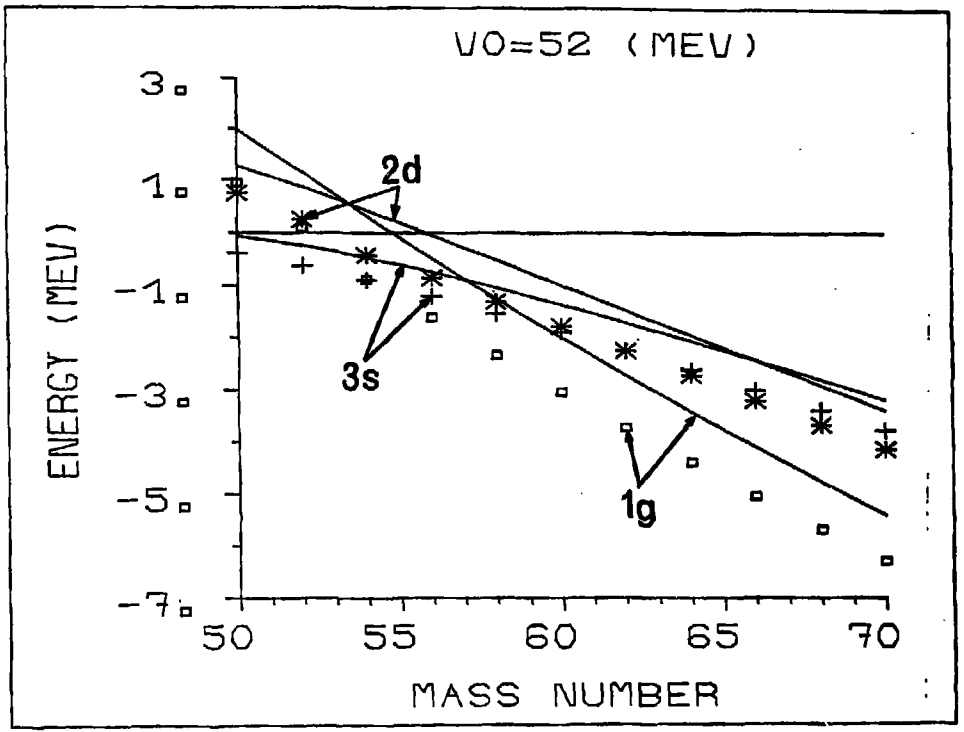

Fig. 14